J Mater Sci: Mater Med (2014) 25:515–525
DOI 10.1007/s10856-013-5072-5

Differentiation of human mesenchymal stem cells on plasma-treated polyetheretherketone

Jasmin Waser-Althaus · Achim Salamon · Marcus Waser · Celestino Padeste · Michael Kreutzer · Uwe Pieles · Bert Müller · Kirsten Peters

Received: 29 May 2013 / Accepted: 10 October 2013 / Published online: 8 November 2013

Abstract Polyetheretherketone (PEEK) generally exhibits physical and chemical characteristics that prevent osseointegration. To activate the PEEK surface, we applied oxygen and ammonia plasma treatments. These treatments resulted in surface modifications, leading to changes in nanostructure, contact angle, electrochemical properties and protein adhesion in a plasma power and process gas dependent way. To evaluate the effect of the plasma-induced PEEK modifications on stem cell adhesion and differentiation, adipose tissue-derived mesenchymal stem cells (adMSC) were seeded on PEEK specimens. We demonstrated an increased adhesion, proliferation, and osteogenic differentiation of adMSC in contact to plasma-treated PEEK. In dependency on the process gas (oxygen or ammonia) and plasma power (between 10 and 200 W for 5 min), varying degrees of osteogenic differentiation were induced. When adMSC were grown on 10 and 50 W oxygen and ammonia plasma-treated PEEK substrates they exhibited a doubled mineralization degree relative to the original PEEK. Thus plasma treatment of PEEK specimens induced changes in surface chemistry and topography and supported osteogenic differentiation of adMSC in vitro. Therefore plasma treated PEEK holds perspective for contributing to osseointegration of dental and orthopedic load-bearing PEEK implants in vivo.

J. Waser-Althaus · A. Salamon · K. Peters (✉)
Department of Cell Biology, Rostock University Medical Center, Schillingallee 69, 18057 Rostock, Germany
e-mail: kirsten.peters@med.uni-rostock.de

J. Waser-Althaus · B. Müller
Biomaterials Science Center, University of Basel, 4031 Basel, Switzerland

J. Waser-Althaus · M. Waser · U. Pieles
Institute for Chemistry and Bioanalytics, University of Applied Sciences and Arts Northwestern Switzerland, 4132 Muttenz, Switzerland

J. Waser-Althaus · C. Padeste
Laboratory for Micro- and Nanotechnology, Paul Scherrer Institut, 5232 Villigen PSI, Switzerland

M. Kreutzer
Center for Medical Research (ZEMFO), Rostock University Medical Center, 18057 Rostock, Germany

1 Introduction

Polyetheretherketone (PEEK) is a high-temperature thermoplastic used as biomaterial for trauma, orthopedic and in this connection especially spine implants [1]. Owing to the chemical structure, it possesses relatively high mechanical stability as well as chemical and radiation resistance. Neither in vitro nor in vivo cell studies on PEEK showed signs of cytotoxicity, immunogenicity or mutagenicity [2–4]. In contrast to metals, PEEK is radiolucent and magnetic resonance imaging compatible, which allows diagnostic examination in implant's vicinity [4]. Young's modulus E of pure PEEK is between 3 and 4 GPa [5]. To increase elasticity of PEEK implants to that of cortical bone ($\sim$18 GPa), carbon fiber reinforcement was successfully used [3].

PEEK is hydrophobic and exhibits a low surface energy, which limits cell adhesion capacity [6]. Therefore, PEEK has been so far successfully used for applications where implant osseointegration is not essential [1]. Due to its relative inertness, several attempts were made to activate PEEK implant surfaces. Coatings with Ti and hydroxyapatite [2] as well as plasma treatment were shown to be compatible with PEEK [2, 7]. Processing without coating,

i.e. wet chemical activation [7–9] and plasma treatments [7, 10, 11] were shown to be alternatives. Treatment with oxygen and ammonium plasma creates functional groups at the surface of polymers, which can increase the surface energy (hydrophilicity) and modify the surface topography without affecting the bulk properties [12]. Therefore, oxygen and ammonia plasma show promise for surface activation of PEEK [13] potentially replacing elaborate coating techniques. It was shown that plasma treatment generates nanostructures on polymer surfaces such as polydimethylsiloxane [14], polymethyl metacrylate and PEEK [15]. Controlling plasma power and exposure time, nanostructures of defined size can be fabricated by oxygen and ammonia plasma treatments [13].

A decade ago, Zuk et al. [16] characterized a stem cell population within the adipose tissue that is of mesenchymal origin and able to undergo e.g. adipogenic (AS), osteogenic (OS), and chondrogenic differentiation. These cells are termed adipose tissue-derived stem cells (adMSC). Due to their primarily mesenchymal differentiation potential, their frequent occurrence and the ease of harvesting, adMSC are a potential alternative to mesenchymal stem cells (MSC) from bone marrow for utilization in regenerative therapies such as bone and adipose tissue regeneration [17–19].

In recent years, a number of studies demonstrated that the underlying substrate is a critical determinant of stem cell behaviour. The key material properties affecting stem cell or primary cell behaviour have been categorized into elasticity [20], surface morphology on micro- and nanometer scale [21–24] and surface chemistry [25]. Thus, successful adhesion and differentiation of MSC towards osteoblasts would significantly contribute to the development of iso-elastic, coating-free PEEK implants for orthopaedic applications.

In this study, we examined the differentiation of adMSC towards the OS and AS lineage in vitro in dependence of plasma treatment of PEEK substrates. To determine surface activation conditions for optimized cell differentiation, PEEK specimens were oxygen and ammonia plasma-treated using a series of plasma powers.

2 Materials and methods

2.1 Materials

The chemicals, enzymes, antibiotics and biological factors were supplied, if not indicated otherwise, by Sigma-Aldrich (Steinheim, Germany). Cell culture plastics were from Nunc and Greiner (Frickenhausen, Germany).

2.2 PEEK sheet pretreatment

Hot embossing with a HEX03 press (JENOPTIK Mikrotechnik GmbH, Oberkochen, Germany) at a temperature of 160 °C and a pressure of 100 kN served to flatten commercially available amorphous APTIV^{TM} PEEK sheets (Series 2000, Victrex Europa GmbH, Hofheim, Germany) with a thickness of 25 µm between two polished 4-inch silicon wafers. During this process the PEEK changes from amorphous to a partially crystalline state [26].

2.3 Plasma treatment (plasma etching)

Oxygen/argon or ammonia plasma treatments (Piccolo system, Plasma Electronic, Neuenburg, Germany) activated the embossed PEEK sheets. PEEK specimens were placed at the bottom of the plasma chamber (RF-system, 13.56 MHz). Subsequently, the chamber was evacuated, flushed for a period of 5 min with oxygen/argon (200/100 sccm, 99.5/99.2 %, Messer, Lenzburg, Switzerland) or ammonia (200 sccm, 99.98 %, Messer, Lenzburg, Switzerland) and then equilibrated for further 5 min with oxygen/argon (20/10 sscm) or ammonia (30 sccm) gas. The plasma treatments of 5 min using a power of 10–200 W resulted in pressures between 0.5 and 1.8 Pa and bias voltages between 55 and 400 V. Argon was used to support the oxygen plasma.

Since plasma-activated polymer surfaces are subjected to molecular changes termed ageing [27], we performed the presented experiments with the activated PEEK specimens 7 days after plasma treatment.

2.4 Water contact angle measurements

The wettability of (plasma-treated) PEEK was determined with double distilled water (ddH_2O) by the sessile drop contact angle method using a contact angle goniometer (Drop Shape Analysis System PSA 10Mk2, Krüss, Hamburg, Germany). Contact angles were measured 5 s after placing the 4 µL drop at room temperature in triplicate.

2.5 Scanning electron microscopy

The plasma-treated PEEK specimens were coated with Au/Pd (9 nm) during 30 s using a current of 20 mA in a vacuum of 6 Pa (sputter coater Polaron, Thermo VG Scientific, East Grinstead, United Kingdom). Substrate surfaces were investigated with the field emission scanning electron microscope Supra 40 VP (Carl Zeiss, Jena, Germany) at an applied acceleration voltage of 10 kV using an InLens detector.

2.6 Protein adsorption

The protein amount is quantified via the colorimetric conversion of a bichinonic acid Cu^{+} complex in solution. In this manner the protein was quantified directly when adsorbed on the substrate. The PEEK specimens were stamped out in a 12 mm diameter format, the treated side was wetted with phosphate-buffered saline (PBS) and then incubated on a 200 µL drop of 10 % foetal calf serum (FCS, PAN-Biotech GmbH, Aidenbach, Germany) or 10 mg/mL bovine serum albumin (BSA, Cohn fraction V) in PBS for 2 h at 37 °C using the inverted drop method: the 200 µL drop was placed on a parafilm in a wet chamber and the PEEK specimen was placed on the drop with the treated side. The incubated PEEK was subsequently washed with PBS using the inverted drop method to remove excess protein. The specimens were then incubated with 600 µL micro BCA reagent (Thermo Scientific, Rockford, USA) at 60 °C for 1 h and the protein concentration was determined via the optical density at 562 nm.

2.7 Zeta-potential measurements

All streaming potential measurements to determine the zeta potential values were carried out with the Electrokinetic Analyzer (Anton Paar KG, Graz, Austria) and the measuring cell for flat plates as described previously [28].

2.8 XPS measurements

XPS studies were carried out by means of an Axis Nova photoelectron spectrometer (Kratos Analytical, Manchester, England). The spectrometer was equipped with a monochromatic Al Kα ($h\nu = 1{,}486.6$ eV) X-ray source operated at a power of 225 W. The kinetic energy of the photoelectrons was determined with a hemispheric analyser set to a pass energy of 160 eV for the wide-scan spectra and 40 eV for the high-resolution spectra (full-width-at-half-maximum of $Ag3d_{5/2}$ was 1.8 and 0.6 eV, respectively). During the measurements, electrostatic charging of the specimen was overcompensated by means of a low-energy electron source. The peak fitting was performed with the CasaXPS software (Version 2.3.15, Casa Software Ltd.). The energy scale of the spectra was calibrated against the C_{1s} line of aliphatic carbon at $E_b = 285.0$ eV. An iterated Shirley background was subtracted from the spectra. Quantitative elemental compositions were determined from peak areas.

2.9 Cell culture

Human adMSC from liposuction-derived adipose tissue were isolated by collagenase digestion (collagenase NB4 from *Clostridium histiolyticum*, 0.12 PZ units (Wünsch)/mg, 6 mg/mL adipose tissue, Serva, Heidelberg, Germany). The enzymatic digestion was performed for 0.5 h at 37 °C (slight shaking). Afterwards the homogenous solution was filtered through a 100 µm filter (nylon cell strainer, BD Falcon, Heidelberg, Germany) and the resulting cell suspension was washed three times with PBS containing 10 % FCS (PAN, Aidenbach, Germany) and repeated centrifugation at $400 \times g$ for 5 min. The final cell pellet was resuspended in DMEM (Gibco Invitrogen, Karlsruhe, Germany) containing 10 % FCS and antibiotics (final concentration: 100 U/mL penicillin, 100 µg/mL streptomycin, Invitrogen, Germany), seeded in cell culture flasks and cultivated at 37 °C and 5 % CO_2 in a humidified atmosphere. 24 h after cell isolation the CD34-positive subpopulation was isolated by the Dynal® CD34 progenitor cell isolation system (Invitrogen, Karlsruhe, Germany) as described previously [19]. These experiments were conducted with the approval of the ethics committee (Medical Faculty, University of Rostock) and the full consent of the patients.

In the fourth passage seeding of cells into experimentation was done at 20,000 cells per cm^2. Absence of contaminating monocytes/macrophages and endothelial cells was confirmed by flow cytometry (FACSCalibur; BD Biosciences AG, Heidelberg, Germany) proving the absence of $CD14^{+}/CD68^{+}$ (eBioscience, Frankfurt a. M., Germany) and $CD31^{+}$ (Millipore, Schwalbach, Germany) cells, respectively. After seeding, adMSC were cultured until confluence was reached and then stimulated to differentiate using OS differentiation stimulating medium (OS: basal medium plus 0.25 g/L ascorbic acid, 1 µM dexamethasone and 10 mM beta-glycerophosphate) or AS differentiation stimulating medium (basal medium plus 1 µM dexamethasone, 500 µM IBMX, 500 µM indomethacin, 10 µM insulin). For the unstimulated (US) adMSC control cultures the basal medium did not contain any specific differentiation factors. Start of stimulation is termed day zero of experimentation. The plasma treated PEEK specimens were punched out to fit into a 96 well format, sterilized with 70 % ethanol (LiChrosolv, MERCK, Darmstadt, Germany) washed two times with Dulbecco's PBS (without Ca^{2+} and Mg^{2+}, sterile; PAA Laboratories GmbH, Cölbe, Germany), and incubated with medium for 2 h before adMSC seeding. All experiments represented as box plots were performed at least 4 different liposuction-derived adipose tissue donors.

2.10 Cell number quantification

Quantification of adMSC number at the distinct experimental conditions was done indirectly using the basic dye crystal violet [29]. Due to a linear correlation, cell numbers

can indirectly be determined quantifying the optical density of the re-solubilised dye [30]. Briefly, cells were washed with PBS, fixed with 2-propanol (SERVA Electrophoresis GmbH, Heidelberg, Germany), permeabilised (0.05 % Tween 20 in PBS), stained with crystal violet (0.1 % in PBS) for 60 min and washed with ddH_2O. Subsequently, bound crystal violet was dissolved in acetic acid (33 %; Merck KGaA, Darmstadt, Germany), transferred to an optical plate and quantified via its optical density at 600 nm (anthos 2010 optical density microplate reader; anthos Mikrosysteme GmbH, Krefeld, Germany).

2.11 Quantification of alkaline phosphatase (ALPL) activity

ALPL catalyses the hydrolysis of an arylphosphate residue of its synthetic substrate para-nitrophenyl phosphate (pNPP) into the coloured product paranitrophenol [31]. Thus, by quantification of the optical density of the coloured product generated in a given time, the ALPL activity can be determined.

For this analysis cells were washed with Tris-buffered saline, lysed using a detergent- and protease inhibitor-containing buffer (1 % Tween 20 and 100 µM phenylmethanesulfonylfluoride/PMSF (AppliChem GmbH, Darmstadt, Germany) in ddH_2O, incubated with ALPL substrate solution (10 mM pNPP, AppliChem GmbH, Darmstadt, Germany), 100 mM 2-amino-2-methyl-1,3-propanediol and 5 mM $MgCl_2$ (AppliChem GmbH, Darmstadt, Germany) in ddH_2O for 60 min at 37 °C, 5 % CO_2 in a humidified atmosphere. pNPP conversion was stopped using 2 M NaOH, and the optical density of the supernatant was quantified at 405 nm.

2.12 Quantification of extracellular matrix calcium content

Extracellular matrix calcium content was optically quantified using cresolphthalein. In order to quantify only the concentration of calcium ions in solution, magnesium ions have to be masked. This was accomplished by adding the chelating agent 8-hydroxy chinoline [30]. The procedure used was adapted from Proudfoot et al. [32] and involves acidic liberation of calcium ions from the extracellular matrix and subsequent complexation under alkaline conditions. For that purpose, cells were washed with PBS, fixed with 4 % paraformaldehyde (PFA) prewarmed to 37 °C, washed with ddH_2O and then incubated in cresolphthalein buffer (0.1 mg/mL ortho-cresolphthalein complexon, 1 mg/mL 8-hydroxy chinolin and 6 % (v/v) of 37 % HCl in ddH_2O) for 5 min. Then, 2-amino-2-methyl-1-propanol (AMP) buffer (15 % AMP) in ddH_2O, pH = 10.7 was added, and after 20 min, the supernatant was transferred to an optical plate to quantify the optical density at 580 nm.

2.13 Quantification of cellular lipid content

Cellular lipid content was determined using an unmodified lipophilic boron dipyrromethene (Bodipy) dye which dissolves well in cellular neutral lipids, most of which being triglycerides, that build the core of lipid droplets and that are surrounded by a monolayer of phospholipids [33]. Bodipy fluoresces upon excitation at 480 nm or maximal at 493 nm and emits a green fluorescence at 503 nm. Thus, the intensity of the fluorescence emitted by the Bodipy stain is proportional to the total amount of lipid stored within a cell. Briefly, cells were washed with PBS, fixed in 4 % PFA pre-warmed to 37 °C, washed with PBS, incubated in Bodipy solution (1 µg/mL, BODIPY 493/503 (Life Technologies GmbH, Darmstadt, Germany) in 150 mM NaCl) for 10 min in the dark, washed with PBS and subsequently with ddH_2O. The stained cells were investigated under the microscope in standard filter-based fluorescence microscopy (Axio Scope.A1 with AxioCam MRc, both Carl Zeiss MicroImaging GmbH, Göttingen, Germany). To quantify the cellular lipid content, images were converted into linear grey scale mode, the background level was calculated judging the histograms of a group of images of US adMSC, and a PHP-script (www.php.org), complemented by functions of the ImageMagick (www.imagemagick.org) software suite, was used to assess all pixels, cumulated their number as area and their intensity as voxel.

2.14 Live cell staining

Visualization of living cells was done by fluorescence staining with calcein AM. Cells were incubated in basal medium containing calcein AM (Biomol GmbH, Hamburg, Germany) at 1 µM for 15 min at 37 °C, 5 % CO_2 in a humidified atmosphere. Then, this staining solution was exchanged by basal medium, and cells were examined under the microscope in standard filter-based fluorescence microscopy at 496 nm (excitation) and 516 nm (emission).

2.15 Data normalization

To facilitate statistical analysis of the metrical data obtained, data were normalized. To this end, the data, as e.g. ALPL activity, for each adipose tissue donor was collected, and the minimum (x_{min}) and maximum (x_{max}) value for all treatment conditions and time points were determined. The position of a distinct value x obtained for this parameter and individual with respect to the extremes x_{min} and x_{max} was then represented as $x_{norm} = (x - x_{min})/$

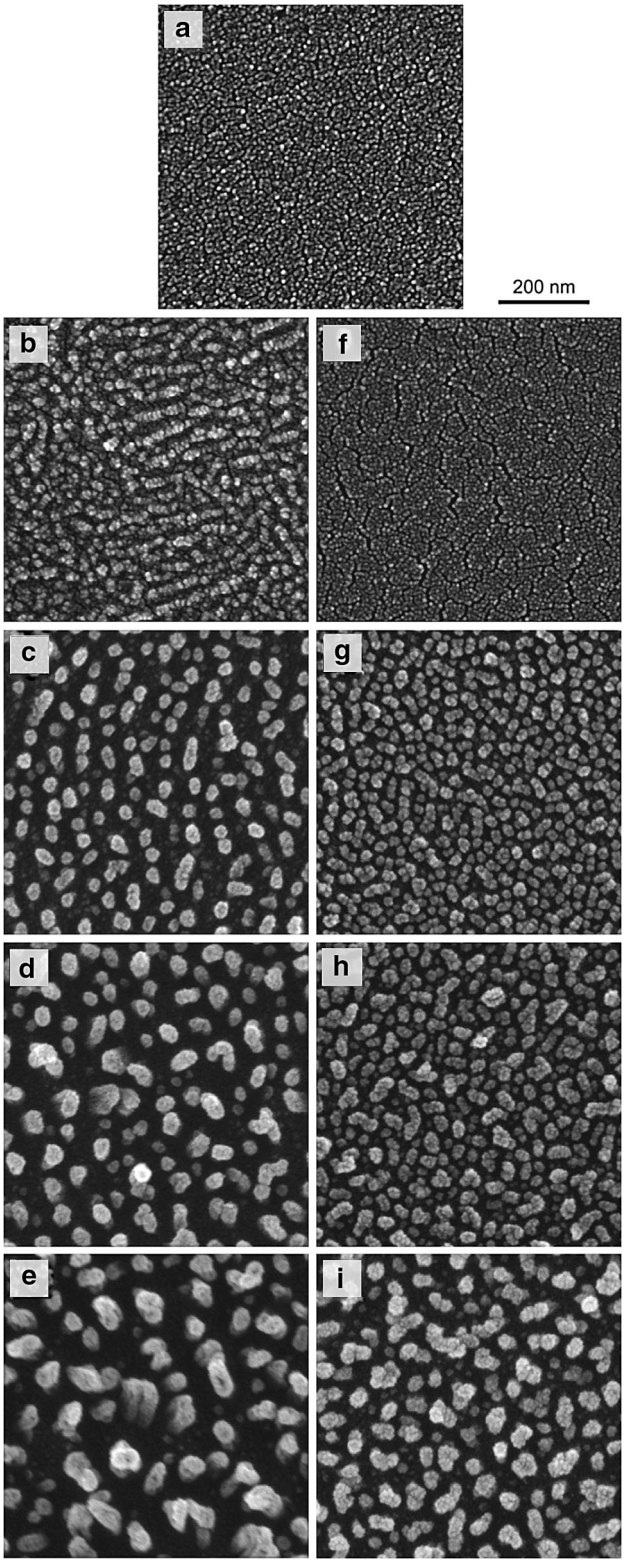

Fig. 1 SEM images of original PEEK (**a**) and 10, 50, 100, 200 W oxygen plasma-treated (**b–e**) and 10, 50, 100, 200 W ammonia plasma-treated (**f–i**) PEEK specimens

($x_{max}-x_{min}$). This operation scales the values obtained for each individual and parameter to a range from zero to one.

2.16 Data presentation

Data are habitually presented as box plots. Here, the solid box represents 50 % of the measured values that assemble around the median indicated by a horizontal line. The box ranges from the 25th to the 75th percentile, i.e. that 25 % of the measured values lay below the lower border of the box and 25 % of them lay above the upper border of the box. Error bars starting below and above the box indicate the 5th and 95th percentile.

2.17 Statistics

All mean values were compared by a non-parametric one-way ANOVA test using Prism 5 (GraphPad Software, Inc., La Jolla, USA). Statistical significance of differences was accepted for $P < 0.05$.

3 Results

3.1 Plasma treatment of PEEK substrates

For activation of the hydrophobic PEEK surface, we applied oxygen and ammonia plasma with powers between 10 and 200 W for a period of 5 min. Both plasma treatments generated a homogenous nanopatterning of the surface with increased roughness. As demonstrated in Fig. 1, oxygen plasma had a stronger effect (Fig. 1b–e) than ammonia plasma (Fig. 1f–i) for identical plasma duration and power. While 10 W oxygen plasma treatment led to pillar-like structures in the range of 10 nm, 200 W treatment resulted in structures with a size of about 50 nm. 200 W ammonia plasma created structures with sizes of about 25 nm.

To further characterize the plasma-treated PEEK surfaces, static water contact angle and protein adsorption measurements were performed. The results of static water contact angle measurements are shown in Fig. 2a. The original PEEK specimen revealed a contact angle of more than 80°. Increasing oxygen plasma power resulted in reduction of contact angles, i.e. being 40° for 10 W and 5° for 200 W. Ammonia plasma treatments also resulted in a decrease of contact angle which, however, increased in dependency of the plasma power, i.e. being 45° for 10 W and 90° for 200 W. In all cases, the amount of adsorbed protein gained with increasing plasma power as illustrated

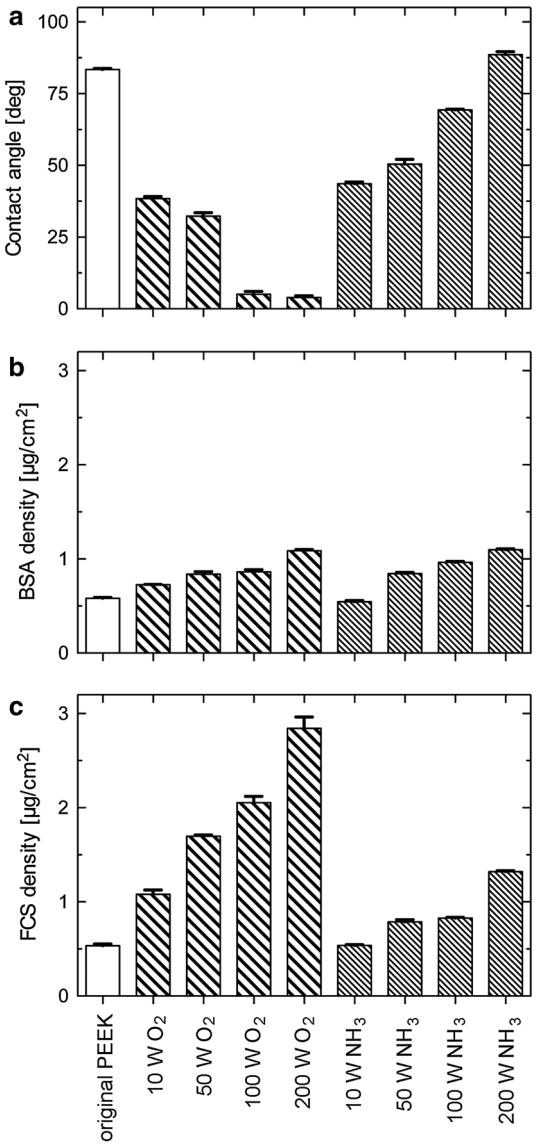

Fig. 2 **a** Static water contact angle of original and of oxygen and ammonia plasma-treated PEEK specimens at day 7 after processing. **b** BSA and **c** FCS adsorption (2 h, 37 °C) of original, oxygen and ammonia plasma-treated PEEK specimens at day 7 after processing, quantified by the micro BCA assay

in Fig. 2b and c. BSA density on oxygen and ammonia plasma-treated specimens as well as FCS on ammonia plasma-treated PEEK was doubled with respect to the original specimens for powers of 200 W, whereas the FCS density on oxygen plasma-treated specimens raised by a factor of six.

Furthermore, the electrochemical surface properties, i.e. the charge of the plasma-treated PEEK specimens, were investigated by zeta-potential measurements via the streaming potential at varying pH-values (Fig. 3). The original PEEK showed a zeta potential of zero at a pH of 3.9, which is the point of zero net charge and therefore

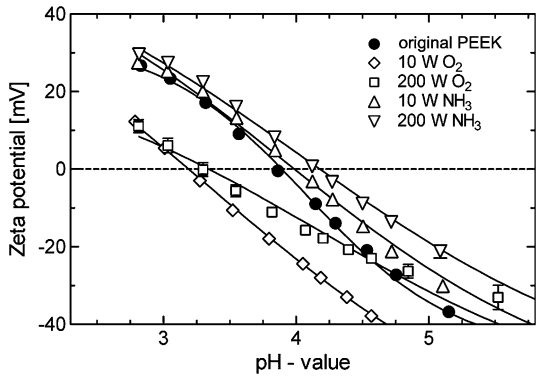

Fig. 3 Zeta-potential measurements of original, oxygen (10 and 200 W) and ammonia plasma-treated (10 and 200 W) PEEK specimens via the streaming potential at given pH-values. The isoelectric points (zeta potential zero) correspond to 3.9, 3.2, 3.3, 4.0, and 4.2, respectively

Table 1 XPS analysis of non-treated and plasma-treated PEEK specimens. Relative concentrations of the detected elements and O/C and N/C ratios as a function of plasma processing parameters

PEEK type	C %	O %	N %	F %	Al %	O/C	N/C
Original PEEK	85.4	13.4	0.1	0.3	0	0.16	0.00
O_2 (0 W plasma)	67.9	25.2	1.2	3.4	1.2	0.37	0.02
O_2 (50 W plasma)	56.7	22.0	1.5	14.6	4.7	0.39	0.03
O_2 (100 W plasma)	45.9	21.8	0.9	22.7	8.0	0.48	0.02
O_2 (200 W plasma)	37.5	25.8	0.8	23.4	11.7	0.69	0.02
NH_3 (10 W plasma)	72.0	11.9	13.1	2.3	0.4	0.17	0.18
NH_3 (50 W plasma)	57.9	10.9	11.8	15.4	4.0	0.19	0.20
NH_3 (100 W plasma)	54.6	15.4	6.7	16.2	7.0	0.28	0.12
NH_3 (200 W plasma)	53.8	19.2	4.5	13.4	8.5	0.35	0.08

corresponds to its isoelectric point (pI). Oxygen plasma treatment resulted in lower pIs, i.e. of 3.2 for a power of 10 W and 3.3 for 200 W, because of the generation of negatively charged groups at the PEEK surface. Ammonia plasma treatment shifted the pI to higher values, i.e. to 4.0 for a power of 10 W and to 4.2 for 200 W.

To gain information about the chemical composition of the plasma-treated PEEK surfaces, XPS spectra were acquired. As summarized in Table 1, there are significant differences between the plasma-treated and the original PEEK surfaces as already shown in more detail elsewhere [34]. The treatment with oxygen plasma led to surface oxidation, as indicated by the O/C ratio which increased steadily with increasing treatment power. Comparably, NH_3-plasma treatment leads to introduction of surface-amino groups. However this effect and therefore the N/C ratio decreased with increasing plasma power. Unexpectedly, the XPS measurements revealed also an enrichment of

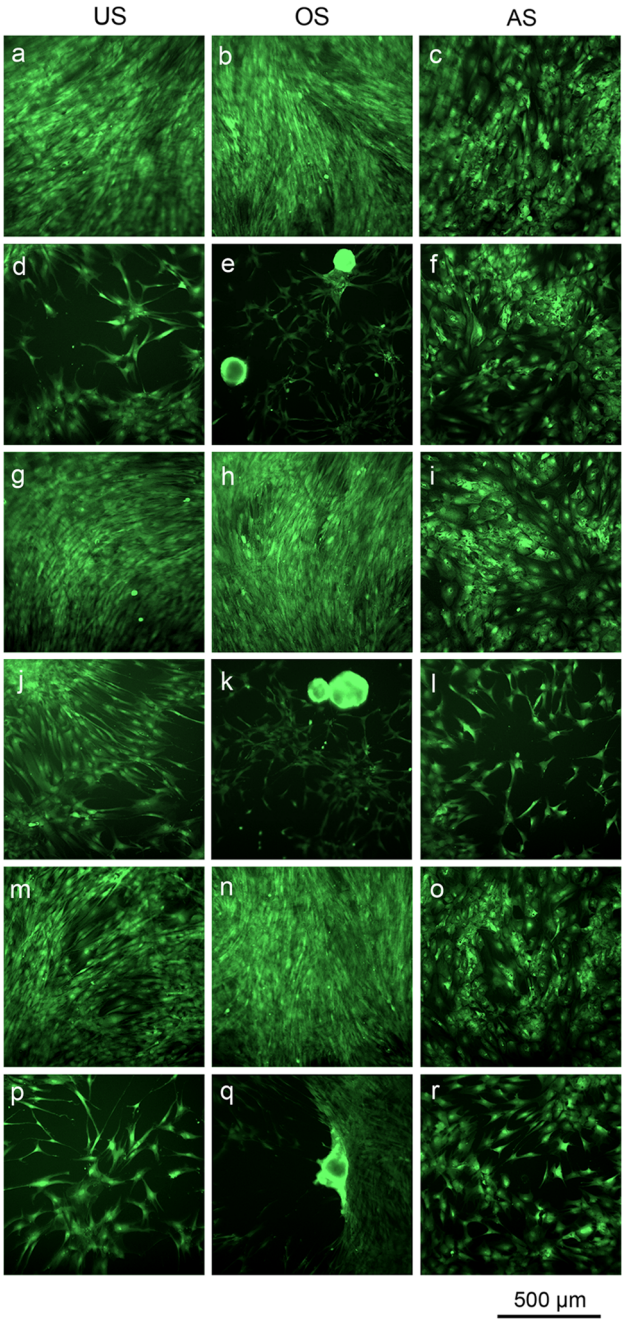

Fig. 4 Calcein AM stain of adMSC at day 14 of culture on TCPS (**a–c**), original PEEK (**d–f**), 10 W oxygen plasma-treated (**g–i**), 200 W oxygen plasma-treated (**j–l**), 10 W ammonia plasma-treated (**m–o**) and 200 W ammonia plasma-treated (**p–r**) PEEK specimens

fluorine and aluminium (present in the oxidized state) on the specimen surfaces at 50–200 W plasma power (Table 1).

3.2 adMSC adhesion and phenotype on plasma-treated PEEK substrates

The effect of the plasma-treated PEEK substrates on adMSC phenotype, vitality, proliferation and differentiation was analysed for US, OS and AS cell culture conditions. The vital staining revealed that the adMSC adhered on standard tissue culture polystyrene (TCPS) and proliferated until confluence under US, OS and AS differentiation conditions at day 14 (Fig. 4a–c). On the original PEEK substrates, adhesion of the adMSC under US and OS conditions was weak and the cells frequently formed spheroids (Fig. 4d, e). adMSC adhesion under AS conditions contrastingly was unaffected in comparison to TCPS (Fig. 4f). Low power oxygen plasma treatment (10 W) resulted in reproducible adMSC adhesion on PEEK (Fig. 4g–i) similar to adhesion on TCPS, whereas high-power oxygen plasma treatment (200 W) allowed only sparse adMSC adhesion for all treatment conditions (Fig. 4j–l). Similar to the oxygen plasma-treated PEEK substrates, adMSC adhered well to the 10 W ammonia plasma-treated PEEK substrates (Fig. 4m–o), but weakly to the 200 W ammonia plasma-treated specimens (Fig. 4p–r). 50 and 100 W oxygen plasma and ammonia plasma-treated specimens gave rise to similar behaviour as noticed for 10 W plasma-treated PEEK specimens (data not shown). Notably, the spheroid formation was only observed up to day 14 of cultivation. After 21 and 28 days, the substrates were completely cell-covered.

adMSC proliferation was quantified for day 14, day 21 and day 28 (results from day 14 see Fig. 5). For all time points measured, the oxygen and ammonia plasma treatments of PEEK specimens up to a power of 100 W led to higher cell numbers than on TCPS and on original PEEK substrates. Under OS conditions, adMSC proliferation was increased, whereas it was halted under AS conditions. We found a dependence of cell number on plasma power for oxygen plasma-treated PEEK substrates under OS conditions, increasing plasma powers resulting in decreasing cell numbers, as qualitatively observed on the live stain images (cp. Fig. 4).

3.3 Differentiation of adMSC on plasma-treated PEEK substrates

OS differentiation was investigated analysing the ALPL activity at day 14 and the mineralization degree at day 28 under OS and US conditions (Fig. 6). ALPL activity was generally increased for OS conditions compared to the US control (Fig. 6a). We observed a plasma power dependent regulation of ALPL activity, being increased on 10 and 50 W plasma-treated PEEK substrates compared to TCPS, the original PEEK substrate and the US controls, but decreased for higher plasma powers. This phenomenon was observed for both reaction gases, while oxygen plasma showed a stronger impact. At day 21 and day 28, such a clear dependency was not found (data not shown).

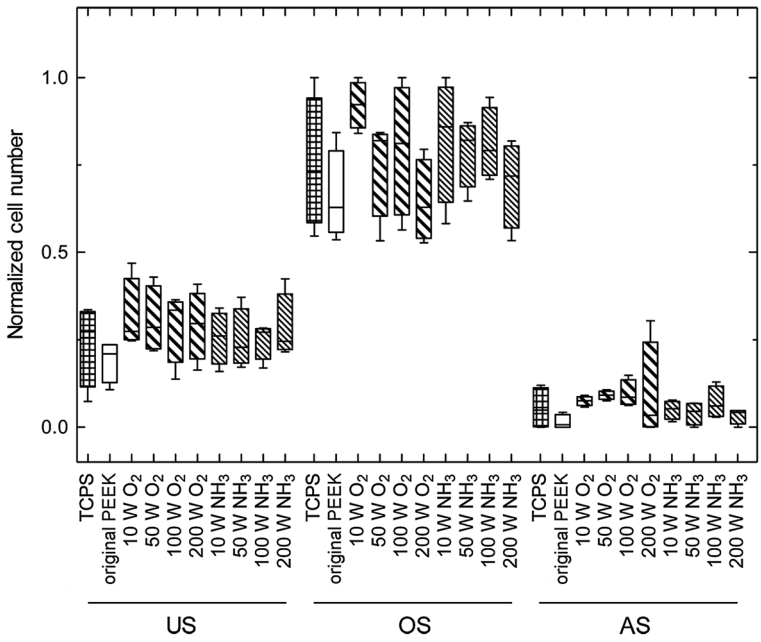

Fig. 5 adMSC quantification at day 14 of culture on TCPS, original PEEK and oxygen and ammonia plasma-treated PEEK specimens with crystal violet. Data were normalized to values between 0 and 1, n = 4

Mineralization was quantified at day 28 (Fig. 6b). Again, we discovered a plasma power dependent regulation of OS differentiation as seen for ALPL activity, since mineralization was increased for the lower plasma power treated PEEK specimens (10 and 50 W) in comparison to the TCPS and the original PEEK substrate controls, but it was decreased for higher plasma power treated PEEK specimens (100 and 200 W).

Furthermore, we investigated the AS differentiation potential of adMSC on plasma-treated PEEK substrates. Cellular lipid accumulation was analysed at day 14 and day 21 under AS and US conditions. Generally, lipid accumulation occurred only under AS conditions. Quantification of cellular lipid content revealed a slight and homogenous increase on ammonia plasma-treated PEEK between 10 and 100 W (approx. 120 % compared to original PEEK), whereas the lipid content was reduced on 200 W ammonia plasma-treated PEEK (approx. 80 %). The lipid accumulation on oxygen plasma-treated PEEK substrates was generally lower compared to original and ammonia plasma-treated PEEK (10–100 W approx. 90 % and 200 W approx. 60 % compared to original PEEK).

4 Discussion

4.1 Surface characteristics

To refine PEEK as suitable polymer for load-bearing implants, its hydrophobic surface needs to be activated to allow cell attachment. Plasma treatments can specifically affect the chemistry and the nanostructure of the substrate's surface [6, 7, 13, 15]. The nanometer-scale topography can be tailored controlling the plasma power, exposure time and process gas composition [13]. Since an increased root-mean-square roughness leads to enhanced protein adsorption, the plasma-induce changes of PEEK surface topography could affect protein adsorption [35]. We could show that plasma treatment strongly impacts water contact angle and protein adsorption. In accordance to literature suggesting that neither extremely hydrophobic nor hydrophilic surfaces bind proteins in conformations accessible for cells [36], adMSC adhesion and proliferation was highest on oxygen and ammonia plasma treated PEEK substrates showing contact angles between 30° and 50°. With increasing plasma power an increase in surface roughness and higher amounts of BSA and FCS were detected. The detected BSA density of 0.6 μg/cm^2 on the original PEEK substrates agrees well with the values calculated for monolayer coverage, which corresponds to 0.7 μg/cm^2 assuming an area of 4 nm × 4 nm per BSA molecule. According to line profiles from AFM measurements, the increase of surface area for the roughest PEEK substrates treated with 200 W plasma is about 15 % for ammonia and about 90 % for oxygen processing compared to the original PEEK. These values for the surface increase was extracted from previous detailed AFM studies on the plasma treated PEEK [13]. While for BSA and FCS one observes a doubling of protein adsorption on 200 W ammonia-treated substrates, 200 W oxygen-plasma led to twofold and sixfold densities for BSA and FCS, respectively, compared to the original PEEK. The consideration of surface enlargement can, therefore, only partly explain the increased protein adsorption. Hence, one may conclude that the

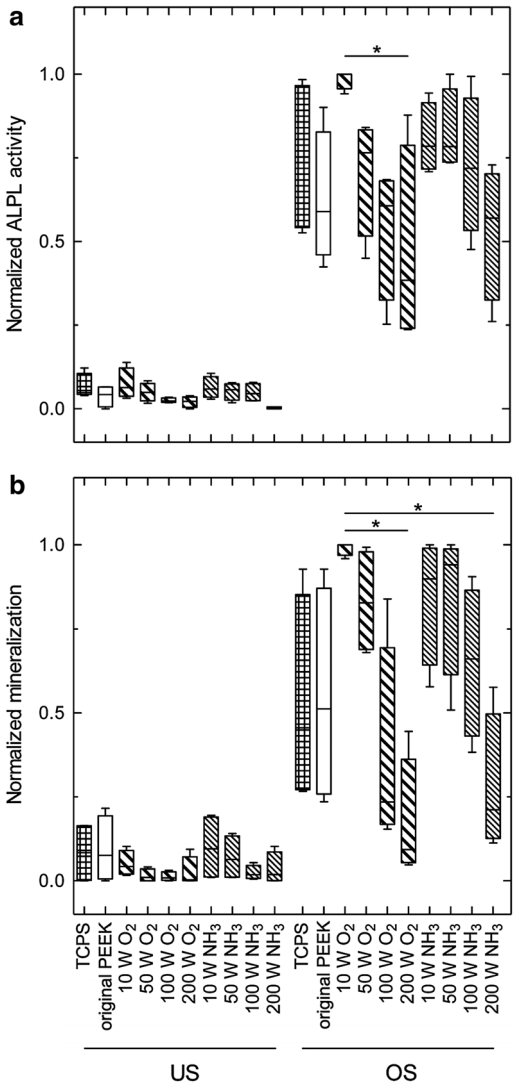

Fig. 6 Osteogenic differentiation of adMSC on TCPS, original, oxygen and ammonia plasma-treated PEEK substrates. **a** ALPL activity at day 14 of culture under US and OS conditions. **b** In vitro mineralization at day 28 under US and OS conditions. Data were normalized to values between 0 and 1, n = 4

nanostructures act as nucleation centres for the proteins, an effect that was described for immunoglobulins and BSA on nanopyramidal surfaces [37, 38]. In contrast to BSA, FCS contains a mixture of proteins, potentially enabling selective protein adsorption. In this context, the local surface charge plays a crucial role. For instance, it was shown that hydroxyapatite functionalized with differently charged amino acids, namely arginine or aspartic acid, selectively bound more BSA or lysozyme in a competitive protein adsorption assay [39]. Oxygen plasma treatments shifted the pI of the PEEK specimens significantly towards the acidic range through creation of negatively charged carboxylic acid or ester groups, whereas ammonia plasma treatments gave rise to a more alkaline pI because of the creation of positively charged amine groups [34]. In accordance to our observations, Safinia et al. [40] noted that air plasma shifted the pI towards the acidic range, whereas ammonia plasma in combination with water treatment resulted in a pI slightly shifted towards the basic pH range.

Interestingly, our XPS measurements revealed a decreasing N/C ratio with increasing ammonia plasma power. High ammonia plasma powers cause etching and loss of NH_2 radicals from the surface, resulting in lower amounts of incorporated nitrogen on the PEEK surface [27]. This may also explain why contact angles increased with increasing plasma power. The higher plasma powers resulted in increasing amounts of fluorine and aluminium on the PEEK surface for both process gases. As one of the starting materials in the production of PEEK is fluorinated, the accumulation of fluorine with increasing plasma power is explained by thermally activated surface segregation of fluorinated residues in the PEEK specimens [41]. The plasma chamber, which is made from aluminium, is most likely the source of the aluminium oxide on the plasma treated specimens. Since Mendonça et al. [42] and Cooper et al. [43] have shown that aluminium oxide or fluoride-containing coatings of titanium implants may enhance OS differentiation we do not expect impairing effects from the accumulation of aluminium and fluorine on our substrates.

4.2 Cellular reactions

Adhesion of adMSC was higher on low power oxygen and ammonia plasma-treated PEEK specimens (10 and 50 W) where the root-mean-squared (RMS) roughness is smaller (average height for oxygen plasma is 9 and 18 nm, for ammonia plasma 3 and 7 nm, respectively) than for the more powerful plasma treatments (i.e. 100 and 200 W) (average height for oxygen plasma is 24 and 37 nm, for ammonia plasma 11 and 13 nm, respectively), according to AFM line scans. Dalby and colleagues have demonstrated that nanostructures in the height-range of 13 nm positively influence fibroblast adhesion and proliferation, whereas 95 nm high nanostructures have a negative effect [23, 44]. PEEK substrates that supported adMSC adhesion also induced pronounced OS differentiation (i.e. 10 and 50 W oxygen and ammonia plasma-treated PEEK), whereas PEEK substrates that impaired adMSC adhesion also impaired OS differentiation (i.e. 200 W oxygen and ammonia plasma-treated PEEK). This correlation was first described by Spiegelman and Ginty [45]. These authors examined a dependency of the differentiation characteristics of the AS cell line 3TE-F442A on the adhesion substrate and demonstrated that well-spread cells exhibited less AS differentiation than cells with weaker adhesion. McBeath et al. [22] showed that bone marrow MSC that

were allowed to adhere, flatten, and spread underwent osteogenesis, while unspread, round cells became adipocytes. These cell shape induced differentiation changes of MSC were accounted to the signalling of the small GTPase RhoA, which is involved in the regulation of cytoskeletal tension [22]. Furthermore, our experimental findings correlate well with the observations of Poulsson and Richards, who found that human primary osteoblast-like cells show higher levels of in vitro mineralization on oxygen plasma treated PEEK in comparison to unmodified PEEK surfaces [6].

Noticeably, while US and osteogenically stimulated adMSC did not adhere comprehensively on original PEEK, adipogenically stimulated adMSC exhibited a homogenous growth even on original PEEK. These differences in adhesion of adMSC could evolve from the mode of action of a ligand-activated transcription factor termed peroxisome proliferator-activated receptor γ (PPARγ) that is activated in AS stimulation [46]. Activation of PPARγ increases cellular motility via changes in cytoskeletal organization [47], i.e. the increased adhesion observed for adipogenically stimulated adMSC could have resulted from reduced cytoskeletal tension due to activation of PPARγ.

Although the ammonia and oxygen plasma-treated PEEK specimens significantly differ with respect to surface chemistry and roughness, adMSC adhesion, proliferation and differentiation were largely similar. This raises the question whether surface nanostructure or surface chemistry dominates the observed adMSC differentiation. The nanostructure may be of secondary importance, as the nanostructures on oxygen and ammonia plasma-treated substrates significantly differ in height and density and as there is no direct correlation with the protein adsorption. The chemical modification of the PEEK surfaces through the oxygen and ammonia plasma treatments, as revealed by the XPS and contact angle measurements, is complex. The electrochemical properties showed reaction gas dependent but not plasma power dependent effects. Therefore, we have to conclude that both surface chemistry and nanostructuring lead to the positive effect on adMSC differentiation. 10 and 50 W oxygen and ammonia plasma-treated PEEK surfaces proved to be suitable substrates to promote OS differentiation in vitro.

5 Conclusion

Activation of PEEK surfaces using 10 and 50 W oxygen and ammonia plasma treatments (exposure time 5 min) generated nanostructured substrates allowing extensive adMSC adhesion, proliferation, and OS differentiation compared to the original PEEK. These in vitro data indicate that plasma-treated PEEK-implants are osteopromotive in vitro and thus may permit osseointegration of these isoelastic, magnetic resonance imaging compatible, and X-ray transparent load-bearing implants in vivo.

Acknowledgments This work was funded by the Swiss Nanoscience Institute (project 6.2), the Rector's Conference of the Swiss Universities (CRUS) and the Federal State of Mecklenburg-Vorpommern, Germany. The authors thank Stefanie Adam (Department of Cell Biology, Rostock University Medical Center, Germany) for her excellent technical assistance and Dr. med. habil. Jürgen Weber (Ästhetikklinik Rostock, Germany) for providing liposuction tissue. Further acknowledgements go to Prof. Dr. Dieter Scharnweber (Technical University Dresden, Germany) and Anja Caspari (Leibnitz Institute for Polymer Research, Dresden, Germany) for support with the zeta-potential measurements and to Dr. Roman Heuberger (RMS Foundation, Bettlach, Switzerland) for the XPS measurements and related data analysis. We thank Victrex for kindly providing us with APTIV™ PEEK sheets.

References

1. Kurtz SM, Devine JN. PEEK biomaterials in trauma, orthopedic, and spinal implants. Biomaterials. 2007;28(32):4845–69. doi:10.1016/j.biomaterials.2007.07.013.
2. Cook SD, Rust-Dawicki AM. Preliminary evaluation of titanium-coated PEEK dental implants. J Oral Implantol. 1995;21(3):176–81.
3. Skinner HB. Composite technology for total hip-arthroplasty. Clin Orthop Relat Res. 1988;235:224–36.
4. Toth JM, Wang M, Estes BT, Scifert JL, Seim HB 3rd, Turner AS. Polyetheretherketone as a biomaterial for spinal applications. Biomaterials. 2006;27(3):324–34. doi:10.1016/j.biomaterials.2005.07.011.
5. Ratner BD, Hoffman AS, Schoen FJ, Lemons JE. Biomaterials science: an introduction to materials in medicine. San Diego: Academic Press; 1996.
6. Poulsson AHC, Richards GR. Surface modification techniques of polyetheretherketone, including plasma surface treatment. In: Kurtz SM, editor. PEEK biomaterials handbook. 1st ed. Waltham: William Andrew/Elsevier Inc.; 2012. p. 145–61.
7. Ha SW, Gisep A, Mayer J, Wintermantel E, Gruner H, Wieland M. Topographical characterization and microstructural interface analysis of vacuum-plasma-sprayed titanium and hydroxyapatite coatings on carbon fibre-reinforced poly(etheretherketone). J Mater Sci. 1997;8(12):891–6. doi:10.1023/A:1018562023599.
8. Noiset O, Schneider YJ, Marchand-Brynaert J. Fibronectin adsorption or and covalent grafting on chemically modified PEEK film surfaces. J Biomater Sci Polym Ed. 1999;10(6):657–77.
9. Noiset O, Schneider YJ, Marchand-Brynaert J. Adhesion and growth of $CaCo_2$ cells on surface-modified PEEK substrata. J Biomater Sci Polym Ed. 2000;11(7):767–86.
10. Briem D, Strametz S, Schroder K, Meenen NM, Lehmann W, Linhart W, et al. Response of primary fibroblasts and osteoblasts to plasma treated polyetheretherketone (PEEK) surfaces. J Mater Sci. 2005;16(7):671–7. doi:10.1007/s10856-005-2539-z.
11. Schroder K, Meyer-Plath A, Keller D, Ohl A. On the applicability of plasma assisted chemical micropatterning to different polymeric biomaterials. Plasmas Polym. 2002;7(2):103–25. doi:10.1023/A:1016239302194.
12. Chan CM, Ko TM, Hiraoka H. Polymer surface modification by plasmas and photons. Surf Sci Rep. 1996;24(1–2):3–54.
13. Althaus J, Padeste C, Köser J, Pieles U, Peters K, Müller B. Nanostructuring polyetheretherketone for medical implants. Eur J Nanomed. 2012;4(1):7–15. doi:10.1515/ejnm-2011-0001.

14. Vlachopoulou ME, Tserepi A, Beltsios K, Boulousis G, Gogolides E. Nanostructuring of PDMS surfaces: dependence on casting solvents. Microelectron Eng. 2007;84(5–8):1476–9. doi:10.1016/j.mee.2007.01.169.
15. Tsougeni K, Vourdas N, Tserepi A, Gogolides E, Cardinaud C. Mechanisms of oxygen plasma nanotexturing of organic polymer surfaces: from stable super hydrophilic to super hydrophobic surfaces. Langmuir. 2009;25(19):11748–59. doi:10.1021/La901072z.
16. Zuk PA, Zhu M, Mizuno H, Huang J, Futrell JW, Katz AJ, et al. Multilineage cells from human adipose tissue: implications for cell-based therapies. Tissue Eng. 2001;7(2):211–28. doi:10.1089/107632701300062859.
17. Rider DA, Dombrowski C, Sawyer AA, Ng GH, Leong D, Hutmacher DW, et al. Autocrine fibroblast growth factor 2 increases the multipotentiality of human adipose-derived mesenchymal stem cells. Stem Cells. 2008;26(6):1598–608. doi:10.1634/stemcells.2007-0480.
18. Levi B, Nelson ER, Li SL, James AW, Hyun JS, Montoro DT, et al. Dura mater stimulates human adipose-derived stromal cells to undergo bone formation in mouse calvarial defects. Stem Cells. 2011;29(8):1241–55. doi:10.1002/Stem.670.
19. Peters K, Salamon A, Van Vlierberghe S, Rychly J, Kreutzer M, Neumann HG, et al. A new approach for adipose tissue regeneration based on human mesenchymal stem cells in contact to hydrogels-an in vitro study. Adv Eng Mater. 2009;11(10):B155–61. doi:10.1002/adem.200800379.
20. Engler AJ, Sen S, Sweeney HL, Discher DE. Matrix elasticity directs stem cell lineage specification. Cell. 2006;126(4):677–89. doi:10.1016/j.cell.2006.06.044.
21. Dalby MJ, Gadegaard N, Tare R, Andar A, Riehle MO, Herzyk P, et al. The control of human mesenchymal cell differentiation using nanoscale symmetry and disorder. Nat Mater. 2007;6(12):997–1003. doi:10.1038/nmat2013.
22. McBeath R, Pirone DM, Nelson CM, Bhadriraju K, Chen CS. Cell shape, cytoskeletal tension, and RhoA regulate stem cell lineage commitment. Dev Cell. 2004;6(4):483–95. doi:10.1016/S1534-5807(04)00075-9.
23. McNamara LE, McMurray RJ, Biggs MJ, Kantawong F, Oreffo RO, Dalby MJ. Nanotopographical control of stem cell differentiation. J Tissue Eng. 2010;2010:120623. doi:10.4061/2010/120623.
24. Kolind K, Leong KW, Besenbacher F, Foss M. Guidance of stem cell fate on 2D patterned surfaces. Biomaterials. 2012;33(28):6626–33. doi:10.1016/j.biomaterials.2012.05.070.
25. Anselme K, Ponche A, Bigerelle M. Relative influence of surface topography and surface chemistry on cell response to bone implant materials. Part 2: biological aspects. Proc Inst Mech Eng H. 2010;224(H12):1487–507. doi:10.1243/09544119jeim901.
26. Althaus J, Deyhle H, Bunk O, Kristiansen PM, Müller B. Anisotropy in polyetheretherketone films. J Nanophotonics. 2012;6(63510):1–11. doi:10.1117/1.JNP.6.063510.
27. d'Agostino R, Favia P, Kawai Y, Ikegami H, Sato N, Arefi-Khonsari F. Advanced plasma technology. Weinheim: Wiley-VCH; 2008.
28. Grundke K, Jacobasch HJ, Simon F, Schneider S. Physicochemical properties of surface-modified polymers. J Adhes Sci Technol. 1995;9(3):327–50. doi:10.1163/156856195x00536.
29. Noeske K. Die Bindung von Kristallviolett an Desoxyribonukleinsaure—Cytophotometrische Untersuchungen an normalen und Tumorzellkernen. Histochemie. 1966;7(3):273–87.
30. Sarkar BC, Chauhan UP. A new method for determining micro quantities of calcium in biological materials. Anal Biochem. 1967;20(1):155–66.
31. Montalibet J, Skorey KI, Kennedy BP. Protein tyrosine phosphatase: enzymatic assays. Methods. 2005;35(1):2–8. doi:10.1016/j.ymeth.2004.07.002.
32. Proudfoot D, Skepper JN, Hegyi L, Bennett MR, Shanahan CM, Weissberg PL. Apoptosis regulates human vascular calcification in vitro—evidence for initiation of vascular calcification by apoptotic bodies. Circ Res. 2000;87(11):1055–62.
33. Spandl J, White DJ, Peychl J, Thiele C. Live cell multicolor imaging of lipid droplets with a new dye, LD540. Traffic. 2009;10(11):1579–84. doi:10.1111/j.1600-0854.2009.00980.x.
34. Althaus J, Urwyler P, Padeste C, Heuberger R, Deyhle H, Schift H, et al. Micro- and nanostructured polymer substrates for biomedical applications. Proc SPIE. 2012;8339:83390Q. doi:10.1117/12.915235.
35. Rechendorff K, Hovgaard MB, Foss M, Zhdanov VP, Besenbacher F. Enhancement of protein adsorption induced by surface roughness. Langmuir. 2006;22(26):10885–8. doi:10.1021/la0621923.
36. Altankov G, Groth T. Reorganization of substratum-bound fibronectin on hydrophilic and hydrophobic materials is related to biocompatibility. J Mater Sci. 1994;5(9–10):732–7.
37. Müller B. Natural formation of nanostructures: from fundamentals in metal heteroepitaxy to applications in optics and biomaterials science. Surf Rev Lett. 2001;8(1–2):169–228. doi:10.1142/S0218625X01000859.
38. Muller B, Riedel M, Michel R, De Paul SM, Hofer R, Heger D, et al. Impact of nanometer-scale roughness on contact-angle hysteresis and globulin adsorption. J Vac Sci Technol B. 2001;19(5):1715–20.
39. Lee WH, Loo CY, Van KL, Zavgorodniy AV, Rohanizadeh R. Modulating protein adsorption onto hydroxyapatite particles using different amino acid treatments. J R Soc Interface. 2012;9(70):918–27. doi:10.1098/rsif 2011.0586.
40. Safinia L, Datan N, Hohse M, Mantalaris A, Bismarck A. Towards a methodology for the effective surface modification of porous polymer scaffolds. Biomaterials. 2005;26(36):7537–47. doi:10.1016/j.biomaterials.2005.05.078.
41. Iyengar DR, Perutz SM, Dai CA, Ober CK, Kramer EJ. Surface segregation studies of fluorine-containing diblock copolymers. Macromolecules. 1996;29(4):1229–34.
42. Mendonca G, Mendonca DBS, Simoes LGP, Araujo AL, Leite ER, Duarte WR, et al. Nanostructured alumina-coated implant surface: effect on osteoblast-related gene expression and bone-to-implant contact in vivo. Int J Oral Maxillofac Implant. 2009;24(2):205–15.
43. Cooper LF, Zhou YS, Takebe J, Guo JL, Abron A, Holmen A, et al. Fluoride modification effects on osteoblast behavior and bone formation at TiO2 grit-blasted c.p. titanium endosseous implants. Biomaterials. 2006;27(6):926–36. doi:10.1016/j.biomaterials.2005.07.009.
44. Dalby MJ, Riehle MO, Johnstone HJ, Affrossman S, Curtis AS. Polymer-demixed nanotopography: control of fibroblast spreading and proliferation. Tissue Eng. 2002;8(6):1099–108. doi:10.1089/107632702320934191.
45. Spiegelman BM, Ginty CA. Fibronectin modulation of cell-shape and lipogenic gene-expression in 3t3-adipocytes. Cell. 1983;35(3):657–66.
46. Lazar MA. PPAR gamma, 10 years later. Biochimie. 2005;87(1):9–13. doi:10.1016/j.biochi.2004.10.021.
47. Chen L, Necela BM, Su WD, Yanagisawa M, Anastasiadis PZ, Fields AP, et al. Peroxisome proliferator-activated receptor gamma promotes epithelial to mesenchymal transformation by rho GTPase-dependent activation of ERK1/2. J Biol Chem. 2006;281(34):24575–87. doi:10.1074/jbc.M604147200.